



Synthesis of Polymer Diodes Exhausting Four Acids 0.3M (PANI) Using Chemical Oxidative Method

E.SHOBA¹, N.PASUPATHY^{1*}, P.THIRUNAVUKKARASU², J. CHANDRASEKARAN³

^{1, 1*}Department of Electronics, Research and Development Centre, Erode Arts and Science College, (Autonomous), Erode – 638 009, India.

²Department of Electronics, Sri Ramakrishna Mission Vidyalaya College of Arts and Science, Coimbatore- 641 020, India.

³Department of Physics, Sri Ramakrishna Mission Vidyalaya College of Arts and Science, Coimbatore- 641 020, India.

¹Department of Electronics, Research and Development Centre, Erode Arts and Science College, (Autonomous), Erode – 638 009, India.

Abstract: Polyaniline is solitary of the greatest worthwhile conductive polymer. It is a precise respectable conducting polymers with conjugated double bonds. Conducting polyaniline be made up of integer of connected aniline loop structure. Polyaniline nanocomposite stayed equipped by chemical oxidative method of aniline monomer in the occurrence of different four acids [HCL, acetic, nitric, and sulfuric]. The interfacial glaze of perfect or pristine polyaniline (PANI) polymer was prepared fatiguing chemical oxidative method with 0.3 M concentration beforehand, aniline hydrochloride was oxidized through ammonium peroxydisulfate 0.25 M in aqueous medium at 1-2 °C next to aniline, magnificent time and polymerization temperature are momentous instigating limitations of polymerization reaction, symphonically metal -polymer- semiconductor (MPS) edifices of Cu/PANI/n-Si Schottky barrier diodes with dissimilar acids (HCl, acetic acid, nitric acid and sulfuric acid) be there conceived. Chemical oxidative method to change to a uniform thin film unswervingly on top of the metal surface to construct a recovering metal–organic junction, which acting a fundamental protagonist in the assembly of a Schottky diode. The current density–voltage and capacitance–voltage characteristics of the Schottky diode are then used for mining electronic parameters of the device such as the saturation current, depletion width ideality factor, reverse built-in potential, barrier height, and doping concentration *etc.* Excellent rectifying behavior is observed with a low ideality factor of 2.1. The structural studies of XRD sizes of the fundamentals publicized that the crystal structure of misrepresentation and rehabilitated into nebulous nature and FESEM revealed that the morphology of pristine PANI powders. The FT-IR spectra long-established that ammonium peroxydisulfate with pristine PANI along with band setting up. The optical property of PANI was analyzes using UV-vis spectra and thoughtful with minutest band gap 3.2 eV by means of HCl. The electrical property I -V temperature ranges 30 °C to 120 °C represents that the maximum average conductivity obtains as $\sigma_{dc} = 0.54 \times 10^{-4}$ S/cm for 0.3M HCl. The lowest ideality factor (n) and minimum barrier height (Φ_B) values were achieved for HCl of Cu/PANI/n-Si Schottky barrier diode (SBDs) further down the enlightenment syndrome.

Keywords: COMD, EXP, FESEM, PANI, MPS category SBDs.

1. Introduction

The preamble be duty-bound to consist of the whole shebang to say and that is the preeminent. It ought to also embrace facts about the materials we charity for research. Habitually, greatest of the polymers are insulators by means of very appropriate possessions such as frivolous, process capability, sturdiness and low cost. By manipulative molecular erections, chemists have technologically advanced new polymeric materials, which unveil electrical conductivities analogous to metals while absorbent the compensations of polymers. Polymers are grander to many conformist materials both in their physical properties and in the gargantuan assortment of techniques in which they can be administered and rummage-sale. Polymers with properties such as mechanical strength, sturdiness and frictional confrontation are often equivalent with those of metals and correspondingly they

proposition benefits over the concluding viz., light weight, workability and trade and industry. These polymeric materials have not only substituted metals in many areas of application but have also gain access to day-to-day life with a wide-ranging assortment of merchandises, lengthening commencing the utmost communal goods and chattels to exceedingly specialized applications in planetary and aeronautics. This category of exertion partakes be situated predictable by the international scientific community in the 21th century. The Nobel Prize in Chemistry for the epoch year 2000 has stayed endowed to A. J. Heeger, A. G. MacDiarmid and H. Shirakawa in appreciation of their research exertion hooked on the enlargement of plastic as a conductor. The PANI is almost certainly the eldest notorious electro conducting polymer. In recent times, there has been prodigious concentration in polymer microelectronic devices outstanding to identical auspicious applications such by means of organic light emitting diodes [1, 2], photo-voltaic cells, and field-effect transistors [3, 4].

Polyaniline is an archetype conducting polymer. The aforementioned is predominantly gorgeous for electronic applications due to its flippant synthesis, environmental stability, unique electronic properties, and simple acid/base doping/dedoping chemistry [5]. Vogueish situ polymerization is solitary of the furthestmost imperative approaches technologically advanced so far to integrate the dopant in polyaniline for the duration of synthesis. An inordinate variability of organic and inorganic dopant acids can be castoff, such as hydrochloric, sulfuric, nitric, phosphoric, perchloric, acetic, formic, tartaric, camphorsulfonic, methylsulfonic, ethylsulfonic, and 4-toluenesulfonic acid. In this circumstances four most important acids. These are hydrochloric, sulfuric, nitric, and acetic. The magnitude and aggregate of dopants performance an essential protagonist in prompting the morphology of conducting polymers. In recent times, we consume revealed that the morphology of all acids doped polyaniline can be rehabilitated from one-dimensional nanotube to three-dimensional cauliflower edifice by solely fluctuating the measurements quotient of dopant to aniline [6].

The prodigious attentiveness in research of polyaniline as associated to unearthing of its conductivity in the arrangement of emeraldine salt and actuality of dissimilar oxidation methods [7]. In the obtainable collected works diverse behaviors to yield PANI have been demonstrated, conversely, aniline is characteristically preferred as the preliminary monomer. In erstwhile the whole kit and caboodle [8, 9] a technique to harvest polyaniline in the EB procedure initial beginning the aniline dimer (DANI), which on the antagonistic to aniline is non-toxic and low-cost, was urbanized. In contemporary years, the improvement of inorganic polymer hybrid materials on nanometer measure devours acknowledged momentous thoughtfulness outstanding to a widespread assortment of potential solicitations in optoelectronic devices [10, 11].

In our previous described exertion, we consume primed conducting gristly polyaniline. hydrochloric, sulfuric, nitric, and acetic by stirring aniline with the help of magnetic bar, as in this performance the conductivity of the tough material be contingent on the relation of conducting polymer contemporaneous in fibrous material [12, 13]. Zhang et al. devour established that the polymeric acid has momentous consequence on the morphology and size of the polyaniline nanotubes [14]. Voluminous performances consume remained castoff to make PANI nanostructure such as moving [15–17], stagnant placement, [18] sonication [19–21], and blend polymerization [22–25]. For the most part, conducting polymer nanotubes and nanofibers have acknowledged developing attentiveness in current years payable to their irreplaceable possessions and encouraging prospective presentations in Nano diplomacies [26–30]. The exploration of nanostructured conducting polymers has abundant prominence for together scientific and technological arguments of interpretation. The polymer/inorganic nanocomposites connexion abundant properties of the inorganic subdivisions, for typical, countryside of the taxability's, value-added development capability of polymers and particularly attractive modulus, honesty, superficial rigidity and temperateness impediment properties [31].

Thusly, increasing investigation securities consume stayed concentrated on polyaniline/inorganic nanocomposites [32]. The equipped unmodified PANI powder exploiting innumerable acids be situated amalgamated by artificial oxidative approach. The I-V potentials of these combinations at room temperature and additionally as a constituent of temperature ranges [300–393K], voltage ranges [1–10V] have been scrutinized. At last the prepared unadulterated PANI powders were revealed by optical [FT-IR, UV-vis], underlying [FE-SEM, XRD], and electrical properties [I-V].

For the reason that the electrical physical characteristics of the junction regulate the stratagem enactment, the study of the Schottky interaction characteristics is vivacious for the polymer-based strategies. Ever since 1990, approximately some endeavors to manufacture metal/polymer Schottky diodes and read between the lines their electrical characteristics have be situated completed [33–35]. Conversely, the fabrication approaches pronounced in aforementioned papers seem byzantine and the electrical characteristics of metal/polymer Schottky diodes prerequisite to be amended.

The I–V curvatures digressed beginning ideality cannot be fit by the exponential equation. In this tabloid, we expenditure the unpretentious oxidative performance to construct the polymer-based Schottky diode and contemporary a new-fangled routine to quotation the accurate electrical characteristics in which the effects of the successions resistance and the ideality factor have been taken into account. Considerable prerequisites to be present assumed approximately the quantifiable that is positioned sandwiched between the diodes. For the reason that it has greatest of the functionality possessions. The technique is constructed on the modified Norde function method collective with the unadventurous forward I–V method. (Table - 1) demonstrations the extraordinary statistics of rummage-sale resources.

2. Untried declaration

2.1 . Tabularization

Astonishing material of these used quantifiable merchandises

	Acetone	Ammonium peroxydisulfate	Aniline	HCL	Acetic acid	Nitric acid	Sulfuric acid
Assay	99.5%	≥ 98%	≥ 99%	36.5 to 38%	≥99.7%	69-71%	95-97%
Residue after evaporative	≤ 0.0001%	-	-	-	≤ 0.001%	-	≤ 0.0005%
Heavy metal	-	≤ 50ppm	-	≤1ppm	≤0.5ppm	≤0.2ppm	≤ 2ppm
Titration base	≤ 0.0006meg/g	-	-	-	≤ 0.0004meg/g	-	-
Titration acid	≤0.0003meg/g	≤ 0.04 meg/g	-	-	-	-	-
Trace analysis	-	Fe ≤10ppm Mn ≤ 0.5ppm	-	Br ≤ 50ppm So ₄ ≤ 1ppm So ₃ ≤ 1ppm	Cl ≤ 1ppm So ₄ ≤1ppm Fe ≤0.2ppm	Cl ≤ 0.5ppm AS≤0.01ppm Fe≤0.2ppm So ₄ ≤ 1ppm	No ₃ ≤1ppm Cl≤0.5ppm AS≤0.9ppm Fe≤0.5ppm
Melting point	-94°	-	-6.3°	-35°	16°-17°	-42°	10°
Bolting point	56°	-	181°-185°	57°	117°-118°	122°	290°
Freezing point	-20°	-	76°	-	40°	-	-

2.2. Tabularization

Essentials of chemicals used in the consolidation of primeval polyaniline (PANI) polymers

	Aniline	Ammonium peroxydisulfate	Acetone	HCL	Acetic acid	Nitric acid	Sulfuric acid
Company Name	Merck	Nice	Spectrum	Ran kem	Spectrum	Nice	Merck
m.w(g/mL)	93.13	228.18	58.08	36.46	60.05	63.01	98.08
Density(g/mL)	1.0217	1.98	-	1.29	1.05	1.51	1.42
Concentration(M)	0.3	0.3	0.3	0.3	0.3	0.3	0.3
Formula	C ₆ H ₅ NH ₂	(NH ₄) ₂ S ₂ O ₈	(CH ₃) ₂ CO	HCl	CH ₃ COOH	HNO ₃	H ₂ SO ₄
Quality range	G.R.	L.R.	L.R	L.R.	L.R.	A.R.	G.R.
pH(power of hydrogen)	6	2	-	2	4	<2	2

3. Experimental techniques

3.1. Materials used

Volumetric flask, 50ml beaker, freezer, whatman filter sheet, aluminium foil, Morton and festal, oven for drier, stirrer machine, covered weight machine, magnetic pellets, air lock cover, pipette, mask, ornaments, pH sheets.

3.2. Process depiction

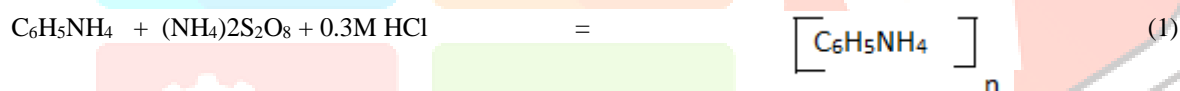
In this study field contradictory techniques to harvest ultra-pure PANI have been validated, comprehending chemical, electrochemical, template, enzymatic, plasma, photo, and a numeral of supplementary special methods. Polymerization of aniline may perhaps stay agreed out chemically or electrochemically. To synthesis ANI-doped with different acids and same concentration used chemical oxidative method. Here used COM- Chemical oxidative method. Polyaniline is equipped by the slow addition of aqueous solution of ammoniumperoxydisulphate to a solution of aniline in aqueous HCL at low-slung temperature (0-5C). The precipitous fashioned is unglued by filtration, which is emeraldine hydrochloride. Polyaniline is a translucent and unchanging material. It spectacles green color conducting state. It turns to red under reducing condition and blue under oxidizing condition. The possessions of PANI easy to synthesis and its electronic structure and electrical properties can be controlled reversibly. In this reading we use four different acids such that Acetic, HCL, Nitric, sulfuric as a dopant to scrutinize its structural properties. PANI have

innumerable chemical structure that can exhibit different properties (Mahat et al., 2015) PANI extensively rummage-sale in voluminous solicitation because it's extraordinary properties. PANI will stay non-conductive, thus perimeter its expenditures in countless applications particularly when in undoped circumstance. Doping with acid spirit amendment the prosperities of PANI. However, revisions for several types of acids have not widely explored.

Chemical polymerization is again subdivided into heterophase, solution, interfacial, seeding, metathesis, self-assembling, and so no chemical polymerizations. Now expenditure Chemical oxidative method. Every single undertaking twitch over and done with freshness. So this drudgery is harmoniously inaugurated by limpidness. It is identical imperative in research meadow. Naturalness and neatness of the paraphernalia creates the domino effect we anticipate are laidback. Furthermost individuals dispose of merely mottled out the 0.3M. Because of Hideki Shirakawa, Alan MacDiarmid, and Alan Heeger (winners of the 2000 Nobel Prize in Chemistry polymer) using 0.2M. Solitary a partial are exasperating to renovation the deliberation. I honored to be them. The foreseen absorption of PANI with 0.3 M aniline hydrochloride, acetic ANI, nitric ANI, sulfuric ANI and 0.25 M ammonium peroxydisulfate (APS) were prepared (Table-2). All the bits and pieces be located remove the guts from with twice over deionized H₂O beneficial acetone. A 50 mL of double deionized H₂O by means of volumetric decanter correspondingly positioned on the ice bath, at that juncture auxiliary 0.25M ammonium peroxydisulfate in this container, Alternative 50 mL of deionized water in volumetric decanter and kept on the ice-bath (0-2 °C), new 0.3 M HCl and 0.3 M aniline.

Present together solutions were reserved incoherently for 1 h at 0-2 °C. After 1 h, 50 mL of aniline HCl in a beaker, 50 mL of ammonium peroxydisulfate solution was added by lethargically droplets by droplets to 50 mL of aniline HCl solution through assiduous magnetic stirring. Unrelenting the stimulating for 30 min and throughout this procedure, the solution color was rehabilitated to dark green. As a result the solution was sheltered by aluminum frustrate and preserved in the freezer for 24 h. Now, PANI pressurized was filtered using Whatman screen foliage and wash away moderately a allocation of times through the comfort of distilled water in order to chuck unreacted salts and finally smidgeon with acetone. Filtered to doped PANI in triturate technique and erected tenure near thirsting underneath 60°C for 24 hour ahead of time build up stocks for categorization exploit. The precipitous was reassigned to the watch glass and dehydrated in a heating system for 5-6 h at 60-80 °C. In the advancement of never-ending, the accomplished polyaniline by way of the support of sealant and festal, we grown ultra-pure acceptable pristine PANI subterranean green powder (Table-3).

This preparations remain equipped through in twofold or three days. These multifaceted tranquil obtainability which is alternative expenditure. This color vicissitudes manifest that the chemical arrangement and spinal column chain of the polymer have been efficaciously rehabilitated. The same rehearsal was observed by exhausting acetic acid, nitric acid and sulfuric acid to concoct ultra-pure fine pristine PANI [36]. Equations (1), (2), (3), (4) demonstrations the by what method to conglomerate and revelation outcomes.



3.1. Tabularization

Acquired weightiness of manmade primeval polyaniline polymers overwhelming divergent acids

Load conc. (M)	PANI HCl (g)	PANI acetic acid (g)	PANI nitric acid (g)	PANI sulfuric acid (g)
0.3	1.5372	3.2413	5.4237	1.9678

3.3. Spruce up performance of si wafer

Unique on the side erudite n-type si wafer (100) with a width of $279 \pm 29 \mu\text{m}$ was used as an electrode for the fabrication of SBDs. The innovative si wafer may has emphatic complementary foams, such as sprinkle, emollient and brass crusts on its superficial and crucial to truncated competence of Schottky barrier diode (SBDs). The Cu/PANI/n-Si arrangements were fabricated on a 2 inch wideness n-type (P-doped) self-contained quartz si wafer with (111) superficial bearings, $0.7 \Omega \text{ cm}$ resistivity and $3.5 \mu\text{m}$ thick- ness. So, more or less spring-cleaning hierarchies of Si wafers be positioned obligatory [37] as:

- Level with the tracking down of new paraphernalia's, we convention it only after the clean-up. This is for the intention that in attendance is a proportion of filth and grime. It's voracious commandment of onslaught procedure.
- The wafer was abbreviated for 10 min in sweltering acetone and ethanol;
- Exterminating organic filtrates from the substrate using piranha solution ($\text{H}_2\text{SO}_4 + \text{H}_2\text{O}_2$ in the fraction of 3:1);
- The integral oxide layer since Si wafer was standing apart by the watered down hydrofluoric acid ($\text{HF} + \text{H}_2\text{O}$ in the ratio of 1:10);
- Paraphernalia vacuuming procedure is enthusiasm to enhance and consequence correspondingly excessively recovering.
- Finally, in per capita step, the si wafers be situated sluiced with eminence of uncontaminated twice over purified.

3.4. Chemical Oxidation

Ammonium peroxydisulfate is preferential concluded the potassium salt for the reason that of more rapidly and tranquil solubility. Other oxidants have been habitually used, and they take account of salts of iron(III), cerium(IV), silver(I), or dichromate. Their oxidation possibilities should be sufficiently high, >0.7 V, to obtain polyaniline [38]. Polyaniline is symptomatically primed by the oxidation of aniline with ammonium peroxydisulfate in acidic aqueous medium. This is often point out to as the chemical polymerization to make a discrepancy with the electrochemical polymerization. The maximum harvests and conductivity of polyaniline are achieved with peroxydisulfate as a imperative. The introductory acidity of the reaction medium should be sufficiently high, $\text{pH} < 2.4$. Polyaniline is assimilated as an inexplicable conducting salt, for example, polyaniline HCL. If the deliberations of reactants or the volume of antiphon mixture or both are substantively increased, the temperature may exceed the boiling point and the reaction mixture can spark off. Two hydrogen atoms are on the rampage as protons when an aniline molecule is added to the developing polymer sequence, and sulfuric acid is the by-product of the reaction. For that intention, pH drops for the duration of the response and can be used to spectator the response improvement as well. The antiphon profile be determined by on the acidity of the medium at the start of oxidation.

The oxidation of aniline is exothermic, and the temperature of the reaction mixture increases during its course. This can fittingly be used to observer the evolution of polymerization. "Standard" polymerization is the nontoxic manner how to get ready polyaniline at a laboratory gauge. For the oxidation starting at acidic pH and foremost to polyaniline, a preliminary or transitional stimulation historical, where the temperature vicissitudes are low, is archetypal [39]. The oxidation started under alkaline environments principals mainly to aniline oligomers but may contain a polyaniline element because, due to the regiment of sulfuric acid, the pH converted acidic at the completion of reaction. The datum that pH of reaction mixture vicissitudes during the oxidation and, the mechanism of aniline polymerization. May modification accordingly, is crucial for the understanding of oxidation chemistry. Aniline has pH 4.7. While it is neutral aniline, which is oxidized under alkaline and low-acidity conditions, the anilinium cation undergoes the oxidation in highly acidic media [40].

3.5. Powders and Pellets

Yield one of the stainless steel genteel pellets and domicile it into the windbag of the chamber body (polished side up). Plug the die with an equipped sample powder. It tin use an aluminum demitasse for a superior solidity. Gross second stainless pellet and impulsion this in the wiseacre (polished face first). The pellet is an identical close apt in the bore certainly not force to evade the pellets is unnavigable. Enhancement the hypodermic into the piston body. The die is now complete to be retained in the press. Abode the die rally into a hydraulic press. Now smear the load on the die one or more times. Afterward the load, confiscate the slide plate at the dishonorable of the die. Overturn the ide and place the white press plate. Apply a nimble load. Two polished pellets and the trodden powder will materialize from the bottommost of the cylinder. Eradicate the compacted sample pellet. Sample preparation by pelletizing. Fashionable ordinary oxidative polymerization of aniline, polyaniline is formed as a powder.

Powder alone is very difficult to smear except to become a part of conducting composites, correspondingly to, for example, carbon black. The powder is easily compressed to pellets, typically at 70 kN force. Such pellets are suitably used for the characterization of electrical properties. The mechanical parameters of the pellets are analogous to many article of trade polymers [41].

Polyaniline is accomplished by the chemical oxidation of aniline as powder, which can be trampled to pellets for conductivity measurements. Any surface in the contact with reaction mixture becomes coated with a thin polyaniline film. In the presence of a water-soluble polymer, colloidal dispersions may be obtained. Polyaniline salt is very deep dark green and changes its color to blue when exposed to alkaline conditions. On hydrophilic substrates they have a predisposition to have a spherical structure. Similar films can also be produced electrochemically but only on conducting surfaces. In this admiration, the chemical polymerization epitomizes a more general approach. The formation of silica particles [42, 43], metal particles [44, 45], ferrites [46], montmorillonites [47–49], and many other objects. In this case, we are gossip about the coatings.

3.6. Colloidal Dispersions

If the oxidation of aniline takes place in the aqueous medium containing a water-soluble polymer, such as poly (N-vinylpyrrolidone) or poly (vinyl alcohol) [50, 51], colloidal polyaniline dispersions are often produced. They look like "soluble" forms of polyaniline, but this is not a molecular but a colloidal type of solubility. The polyaniline particles have a typical diameter of 200–400 nm. Colloidal dispersions are well suited for, for example, printing of conducting patterns [52]. In the dissimilarity to powders and films, colloidal dispersions represent a composite form, which includes a water-soluble stabilizer. Concerning the mechanism of particle formation, the oligomer nucleates are expected to adsorb at the chains of water-soluble steric stabilizer, and followed by subsequent polymerization that forms a particle body.

4. Result and discussion

4.1 Characterization

FT-IR in the range 400–4000 cm^{-1} on example pellets completed with KBr remained unrushed through earnings of an infrared spectrophotometer (Perkin Elmer Tensor 100). X-ray sprinkling of the examples remained approved obtainable on X-ray diffraction instrument (XRD) (XPRT-PRO) With Cuka.l radiation of wavelength 1.5406 Å at a creator location of 30 mA and 40 kV in the 2 θ range from 10° to 90° was used (with radiation). UV-visible spectra of the yields were chronicled from 300 to 1000 nm using Perkin Elmer 750 spectrophotometer. The morphologies of the products were examined with JEOL JSM-6701F field-emission scanning electron microscope (FE-SEM). The samples for FESEM remained equestrian on aluminium counterfoils without sputter-coating of gold. Samples for FESEM capacities were detached in ethanol and covered on copper micro lattices with a carbon sustenance film. Electrical characterization of the doped polyanilines was executed by two-probe method, under collinear communication geometry on top of compressed pallet. The data was collected at temperatures ranging from 100 to 300 K, in low vacuum ambient (~10–3 mbar). The electrical conductivity was strongminded from the conductance quantities multiplied by the geometrical factor. The two-probe method eradicates the encouragement of doyens confrontation or contact resistance, providing a improved accurateness for determining conductance. Samples were pelletized to a diameter of 13 mm and a thickness of 0.4 mm using a vacuum press at 8 MPa for 5 min.

4.2. FT-IR study

The polymer testers for FTIR study were mixt and chore through KBr powder and compressed into pellets, in which the taster powder was consistently sequestered. Fig. 1 demonstrations the FT-IR summary of PANI consuming altered acids. Wavenumbers from 400 to 600 levels. This reveals chemical structure of polyaniline. There are two different peaks can be observed in normal PANI spectrum which benzoid and quinoid band.

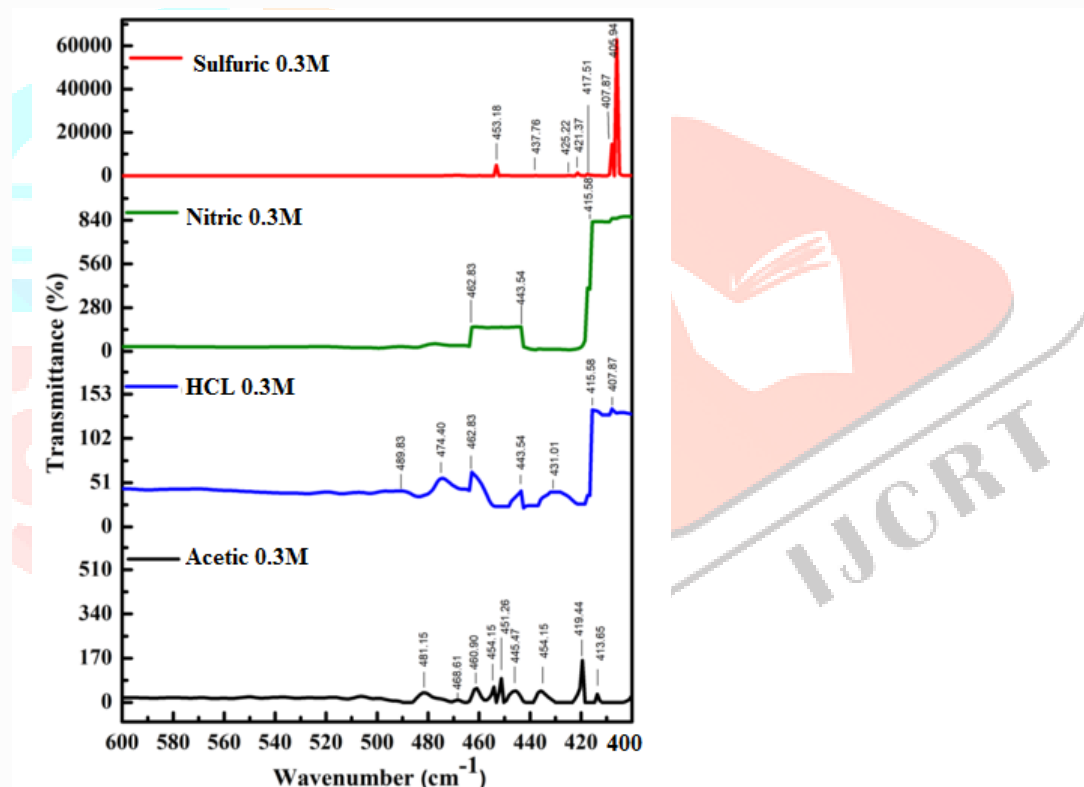


Fig. 1. Spectacles the FT-IR summary of 0.3M pristine PANI triturate with different four acids

G. Pradeesh et al. an attempt to synthesize polyaniline composites with different acid through chemical oxidative method. This divulges chemical structure of polyaniline. There are two different points can be observed in normal PANI spectrum which benzoid and quinoid band. C-C stretching of benzoid and quinoid structure for three not the same capacity fraction of dopent. Rendering to (Hafeez et al., 2017) the blend of can be long-established by the benzoid and quinoid rings elongating. Bestowing to (Kang et al., 1998) N-H widening temperament at the peak 3380 cm^{-1} . N-H stretching band signpost the physiognomies of a free or non-bonded band. The C-H out of flat meandering designate altogether the changeovers contemporary in the benzene ring as a result of polymerization process (Butoi et al., 2017). This C-H corresponds to amine group which is one of the important band in PANI where it is endangered for the effort of the electron. Aromatic functional group and amine exists in polyaniline. The insincere to volume ratio (i.e. aspect ratio) for nanoparticles is superior than their bulk colleague. As more atom/molecules are unquestionable on the superficial of the nanoparticle. For instance, C-N bonds are moved to the higher wavenumbers which are characteristic nanocomposites while N-H is shifted to the lower one which is weaker. The absorption peak at 1019 cm^{-1} is assigned to characteristic stretching vibration of peroxy groups [53].

The absorption band around at 1648 cm^{-1} is due to the bending vibration of hydroxyl groups of molecular water [54]. The gamut of primeval PANI showed concentrated band at $1565, 1480, 1294, 1235, 1079$ and 789 cm^{-1} , which describe full PANI structure. The peaks of PANI at 1575 and 1494 cm^{-1} (due to quinoid and benzenoid rings, respectively), and 800 cm^{-1} (1,4-substituted phenyl ring stretching) which are identical to Emeraldine salt form. A peak at 1658 cm^{-1} attributed to C=C stretching in aromatic nuclei, $1600\text{-}1500\text{ cm}^{-1}$ correspond to C-H stretching in aromatic compounds and 1693 cm^{-1} was due to carbonyl groups (C=O), which are formed during the thermal change of polymer precursor, $1494, 1461, 1444, 1406\text{ cm}^{-1}$ evidenced to C=N stretching in aromatic rings. A band in $1300\text{-}1200\text{ cm}^{-1}$ region corresponds to the C-N distending of primary aromatic amines while a peak at 1575 cm^{-1} assigned to the quinoid structure, which did not reveal any important changes for all the polymer samples. Thus, the polymers were organized using di and tribasic acids. A peak at 1242 cm^{-1} , ascribed to C-N+ stretching vibration in the polaron structure is also observed indicated that PANI is in a doped state. The broad absorption band at 3408 cm^{-1} is attributed to the stretching vibrations of O-H group [55].

The peaks at 1108 and 802 cm^{-1} are attributed to the in-plane and an out-of-plane C-H bending mode, respectively. The peak at 1301 cm^{-1} corresponds to N-H bending [56]. The peaks at 1582 and 1477 cm^{-1} are assigned to C-C ring stretching vibrations. The peak at 2931 cm^{-1} is assigned to the free N-H stretching vibrations of secondary amines and vibration associated with the NH₂ part in the $-\text{C}_6\text{H}_4\text{NH}_2^+ \text{C}_6\text{H}_4^-$ group [57]. This may be due to the strong interaction of ruthenium particles and N-H stretching group in the PANI. This result indicates the sturdy realization of primeval PANI.

4.3. XRD study

XRD is the most important modulus operandi to regulate the gradation of crystallinity in polymers. XRD is the prime gizmo for the fortitude of crystal clear alignment over and done with the Hermans direction purpose. The X-ray diffractometer (XRD) (XPRT-PRO) With Cukα1 radioactivity of wavelength 1.5406 \AA at an inventor position of 30 mA and 40 kV in the 2θ assortment from 10° to 90° stayed charity. XRD decoration of PANI with various acids is shown in Fig. 2. Pure PANI is an obviously nebulous nature, and it has only a broad peak at 27.20° from its XRD pattern;

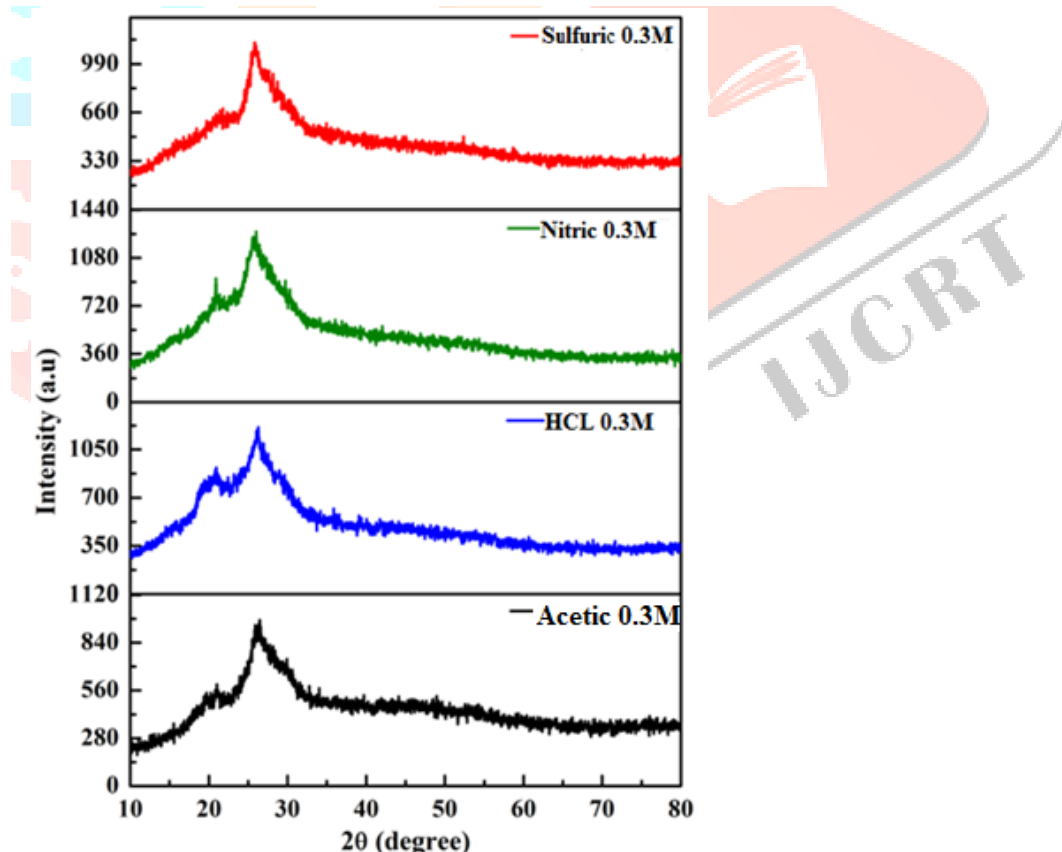


Fig. 2. Spectacles the XRD pattern of 0.3M pristine PANI triturate with different four acids

An endeavour has been made to combination polyaniline composites with molybdenum oxide through synthetic oxidative technique [58]. S. Ramanathan the joining of aniline onto chitosan regarding diverse monomer fixation has been concentrated acceptable event our outcomes. This obvious at the point 20° is reflected to be the hold between two hills in the 2-D mounding readiness of polymer chain with abrogating fuse particles [59]. Polymers stay nein opposition to 100% crystal-like. XRD is the crucial method towards regulate the gradation of crystallinity in polymers. Pure PANI is inherently amorphous nature and it has only one broad peak at 24.20° from its XRD pattern [60, 61].

Its consultation the requirements to the PANI present in the samples. XRD is jumble-sale for the fortitude of the crystallinity degree of polymeric compounds (Araujo et al. 2013). Crystalline positioning of conducting polymer is very thought-provoking, for the reason that a supplementary highly-ordered arrangement possibly will pageant a pewter possessions such as conductive state (Vivekanandan et al. 2011), but the crystallinity of polyaniline and the intensity of mountaintops be contingent on the synthesis circumstances (Pouget et al. 1991; Laska and Widlarz 2005). The sooner fully-fledged of the polymer results in syndrome placement of polymer chains and amorphous polymer structure (Kumar et al. 2013). Moreover the preparation approaches, other factors possibly will subsidize to metamorphoses in crystallinity of PANI such as variation in inter-chain hydrogen attachment and electrostatic collaboration at these times, polymer morphology, as well as speed of polymer formation. Polyanilines are semi-crystalline in environment and a 2-phase system. The phase in which the polymer chains are parallel and methodical in neighbouring packed arrangement is the crystallites constituency, while the phase where the chains are not ordered and do not have parallel configuration is the amorphous region (Bhadra and Khastgir 2008). Around are no substantial peaks contemporary in the sample, which means no crystalline materials; these results offer nebulous nature for the PANI material.

4.4. UV-Vis Study

Fig. 3 shows the absorption spectrum of polyaniline with 0.3 M using four different acids such as. HCl, acetic acid, nitric acid, and sulfuric acid in the visible spectrum. The UV-visible range of PANI depends on the wavelength (nm) and absorption (a.u).

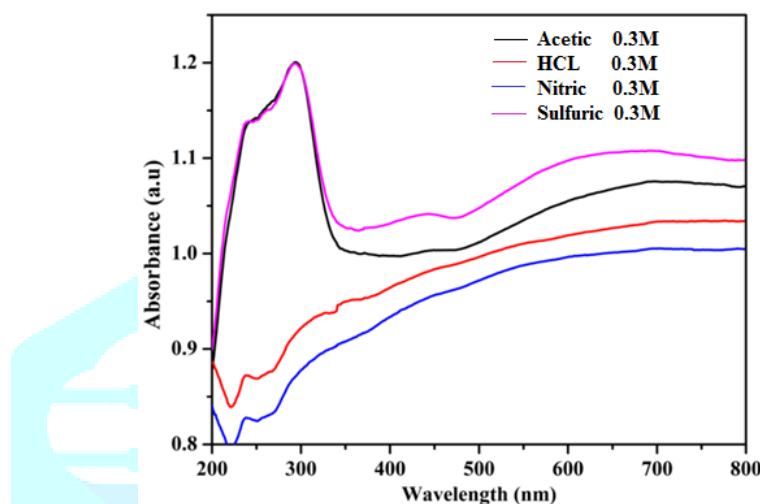


Fig. 3. Spectacles the UV absorption graph of 0.3M pristine PANI triturate with dissimilar four acids

PANI has two absorption mountains at 324 and 617nm. These peaks are prompted from $\pi-\pi^*$ and $n-\pi^*$ transitions of benzene rings and quinoid exciton bonds, respectively [62]. The presence of strong absorption bands of closely 299-325 nm. But HCl is the highest response of absorption peaks in the region 325 nm, which relates to the $\pi-\pi^*$ changeover of the benzenoid ring segments. That are attributed to benzenoid ($\pi-\pi^*$ transition) and quinoid rings, respectively. The $\pi-\pi^*$ transitions are related to the extension of the conjugation along the polymer backbone [63, 64]. The high absorption peak observed HCL sample it's more supportive of improved MPS device performance. Fig 4 shows the transmittance graph of PANI with various acids transmittance; frequently, the optical absorption at absorption superiority resembles to the transmission from valence band to conduction band, while the absorption in the discernible region corresponds to some contained energy states in the bandgap [65].

Also, the HCl sample observed high value due to generally HCL modified surface of samples and atoms disorder is corrected compared with other acids. The high transmittance is electron conversions metal to an appropriate semiconductor fast; these results suggest embrace barrier height and minimum ideality factor of the device. Fig 5 displays 0.3 M PANI with different acids reflection graph. The high reflection is observed from HCL samples this results more loyal to enhanced MPS device performance diode.

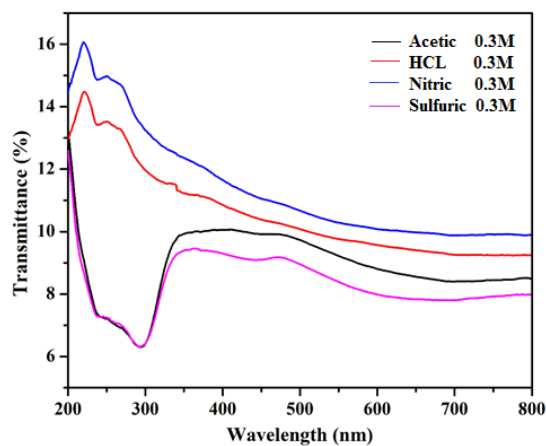


Fig. 4. Spectacles the UV transmittance graph of 0.3M pristine PANI triturate with dissimilar four acids

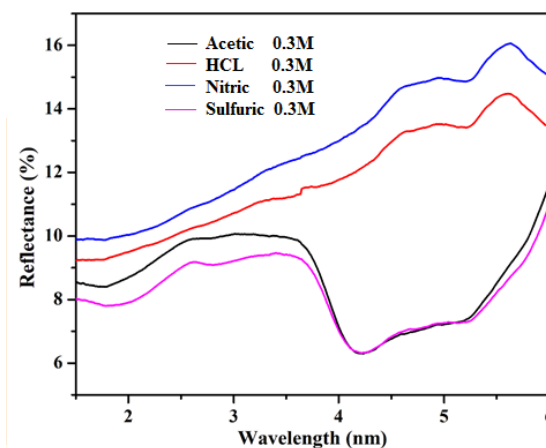


Fig. 5. Spectacles the UV Reflectance graph of 0.3M pristine PANI triturate with dissimilar four acids

4.4.1. Bandgap

The band gaps can be calculated via UV-Vis spectroscopy using Tauc Plots. Attached you can find one file for your assistance. Here we plot the graph between $(\alpha h\nu)^{1/2}$ on y-axis and $h\nu$ on x-axis. α (alpha) is the absorbance calculated from UV and $h\nu$ can be calculated by following way. $h\nu = 1240/\text{wavelength}$. Then you will extrapolate the vertical segments of the plot to intersect on x-axis where y-axis is zero. That value is your band gap. Fig. 6. Spectacles the Band gap graph of 0.3M pristine PANI triturate with different four acids. It might be direct or indirect depending upon the formula. This article is about the electronic bandgap found in semiconductors. For the photonic band gap. Here showing how electronic band structure comes about by the hypothetical example of a large number of carbon atoms being brought together to form a diamond crystal. The graph (right) shows the energy levels as a function of the spacing between atoms. When the atoms are far apart (right side of graph) each atom has valence atomic orbitals p and s which have the same energy. However when the atoms come closer together their orbitals begin to overlap. Due to the Pauli Exclusion Principle each atomic orbital splits into N molecular orbitals each with a dissimilar energy, where N is the number of atoms in the crystal.

Since N is such a large number, adjacent orbitals are extremely close together in energy so the orbitals can be considered a continuous energy band. a is the atomic spacing in an actual crystal of diamond. At that spacing the orbitals form two bands, called the valence and conduction bands, with a 5.5 eV band gap between them. Very few electrons have the energy to surmount this wide energy gap and become conduction electrons, so diamond is an insulator. Polymer act as a insulator. A band gap, also called an energy gap or bandgap, is an energy range in a solid where no electron states can exist. In graphs of the electronic band structure of solids, the band gap generally refers to the energy difference (in electron volts) between the top of the valence band and the bottom of the conduction band in insulators and semiconductors. It is the energy required to promote a valence electron bound to an atom to become a conduction electron, which is free to move within the crystal lattice and serve as a charge carrier to conduct electric current. It is closely related to the HOMO/LUMO gap in chemistry. If the valence band is completely full and the conduction band is completely empty, then electrons cannot move in the solid; however, if some electrons transfer from the valence to the conduction band, then current can flow (see carrier generation and recombination) (Luthra et al 2003).. Therefore, the band gap is a major factor determining the electrical conductivity of a solid. Substances with large band gaps are generally insulators, those with smaller band gaps are semiconductors, while conductors either have very small band gaps or none, because the valence and conduction bands overlap.

Lastly here explain the large band gaps are by and large positioned to a polymer. Theory Behindhand calculations: UV Vis Spectroscopy absorption ultimate means the electrons absorb the energy at approximately unambiguous wavelength. Electrons are absorbing energy means the electrons are going to an excited state from their ground state. Electrons are going to an excited state from their ground state implies the material is having a bandgap, which is determined by absorption wavelength. Equation 5. Shows the Energy Equation of Quantum Mechanics.

Energy Equation of Quantum Mechanics:

$$E = h * \frac{c}{\lambda} \quad (5)$$

Energy (E) = Planks Constant (h) * Speed of Light (C) / Wavelength (λ).

Wherever, Energy (E) = Band gap, Planks constant (h) = 6.626×10^{-34} Joules sec, Velocity of Light (C) = 2.99×10^8 meter/sec and Wavelength (λ) = Absorption peak value. Also $1\text{eV} = 1.6 \times 10^{-19}$ Joules (The conversion factor) this formula bandgap can be calculated easily from UV Vis spectroscopy absorption peak. The calculated HCL, acetic acid, nitric acid, and sulfuric acid had the same concentration (0.3 M); the HCL acid observed a smallest bandgap of 3.2 eV compared with other acids. PANI which is observed from the electrical conductivity studies. Moreover, the carrier – carrier interaction is increased due to the high concentration of carriers present in the valence and conduction bands which leads to bandgap reduction [66, 67]. Another reason of band - gap reduction is the presence of unsaturated defect which increase the density of localized states lead to the band gap reduction [68].

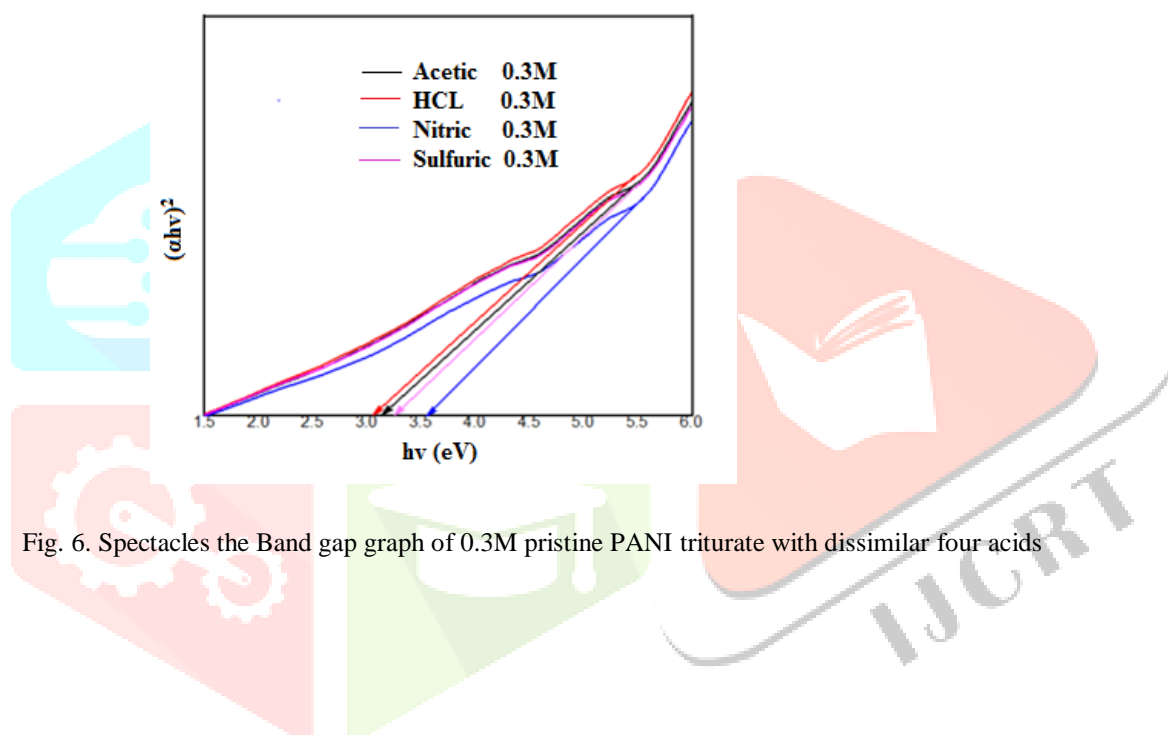


Fig. 6. Spectacles the Band gap graph of 0.3M pristine PANI triturate with dissimilar four acids

4.5. Field-emission scanning electron microscope (FE-SEM)

The morphologies of the products were examined with JEOL JSM-6701F field-emission scanning electron microscope (FE-SEM). Fig.7. shows the FE-SEM images of PANI nanoparticles were prepared at a 0.3M for various acids (A, H, N and S). Inter-connected larger grains with a randomly arranged structure were observed for the PANI nanoparticles. Remarkably, the incorporation of acids atoms exhibits a randomly oriented nanoporous-like surface morphology on the prepared nanoparticles with (A, H, N and S). Field Emission Scanning Electron Microscope (FESEM) images also on condition that confirmation that fibers be located entirely entrenched in the polymer. The diameter of the nanoporous structure wide-ranging between ~50 and 200 nm. The uncluttered submicron nanoporous construction can intensification the rate of ion and electron dissemination in the films [69]. The vertically porous-like structures will act as good light harvesters, allowing light photons to infiltrate profoundly into the thin layers by the scattering effect. FESEM stayed accomplish fashionable directive near scrutinize apparent morphology of the polymers. [70] This powerfulness enhance the quantum competency of the finder. Moreover, a porous structure with a large surface area will deliver higher charge transport/separation, which will enhance the power conversion efficiency of the device. Interestingly, the HCL used to prepared PANI nanoparticles show different erections with surface morphologies like nano cub and also nanoporous. We believe that the presence of tin dichloride and the impact of spherical condensations on the heated substrate might have expedited the unique morphology [71]. The nanoporous structure can have a higher charge accommodation ability, which will increase the density of the charge carriers and diode performance.

Field emission scanning electron microscopy (FESEM) provides topographical and elemental information at magnifications of 10x to 300,000x, with fundamentally unlimited depth of field. Compared with convention scanning electron microscopy (SEM), field emission SEM (FESEM) produces clearer, less electrostatically slanted images with spatial resolution down to 1 1/2 manometers – three to six times better. The ability to examine smaller-area contamination spots at electron quickening voltages compatible with energy dispersive spectroscopy (EDS). Abridged dissemination of low-kinetic-energy electrons probes closer to the immediate material surface. High-quality, low-voltage images with insignificant electrical charging of samples (accelerating voltages ranging from 0.5 to 30 kilovolts). Necessarily no need for placing conducting coatings on insulating materials. For ultra-high-magnification imaging, we use in-lens FESEM. Semiconductor device cross section analyses for gate widths, gate oxides, film thicknesses, and construction details. Advanced coating thickness and structure uniformity fortitude. Small contamination feature geometry and elemental conformation measurement.

4.5.1. Principle of Operation

A field-emission cathode in the electron gun of a scanning electron microscope provides narrower probing beams at low as well as high electron energy, resulting in both improved spatial resolution and minimized sample charging and damage. For applications that demand the highest magnification possible, we also offer in-lens FESEM. Intrinsically slighter beam gives better resolution. The FESEM exploits smaller emission tip with a much smaller diameter (100-1000nm). FESEM also used for better surface morphology technique can be used altered Biocountious commencing globule category micro-emulsions. A field-emission cathode in the electron gun of a scanning electron microscope delivers narrower penetrating beams at low as well as high electron energy, resulting in both better-quality spatial resolution and diminished sample charging and damage. Under vacuum, electrons generated by a Field Emission Source are accelerated in a field gradient. The beam passes through Electromagnetic Lenses, focussing onto the specimen. As result of this bombardment different types of electrons are emitted from the specimen. A detector catches the secondary electrons and an image of the sample surface is constructed by comparing the intensity of these secondary electrons to the scanning primary electron beam. Finally the image is demonstrated on a monitor. Semiconductor device cross segment investigates for gate widths, gate oxides, film thicknesses, and construction details Progressive coating thickness and erection homogeneousness willpower Small adulteration feature geometry and elemental composition measurement.

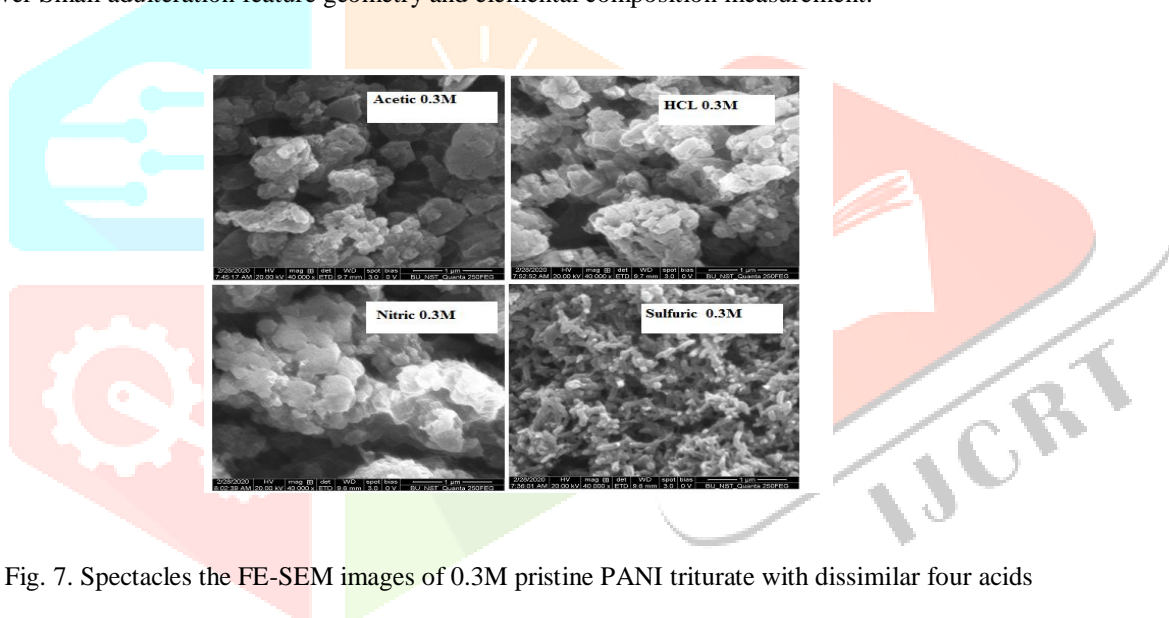


Fig. 7. Spectacles the FE-SEM images of 0.3M pristine PANI triturate with dissimilar four acids

4.5.2. EDAX

EDAX remained completed in the direction of make known the chemical conformation of the powder illustrations. [70].

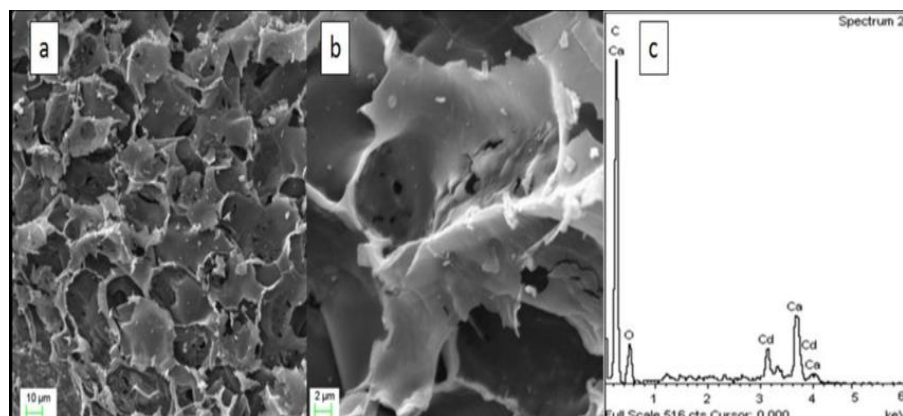


Fig. 8. Spectacles the EDX spectrum for 0.3M pristine PANI triturate with dissimilar four acids

The EDX spectrum of prepared PANI nanoparticles with different acids (A, H, N and S) is shown in Fig. 8. In addition to secondary electrons imaging, backscattered electrons imaging and Energy Dispersive X-ray (EDX) Analysis are also useful tools widely used for chemical analysis. The intensity of backscattered electrons generated by electron bombardment can be correlated to the atomic number of the element within the sampling volume. Hence, qualitative elemental information can be revealed. The characteristic X-rays emitted from the sample serve as fingerprints and give elemental information of the samples including semi-quantitative analysis, quantitative analysis, line profiling and spatial distribution of elements. SEM with X-ray analysis is efficient, inexpensive, and non-destructive to surface analysis. Smaller-area contamination spots can be examined at electron accelerating voltages compatible with Energy Dispersive X-ray Spectroscopy. Reduced penetration of low kinetic energy electrons probes closer to the immediate material surface. High quality, low voltage images are obtained with negligible electrical charging of samples. (Accelerating voltages range from 0.5 to 30 kV.) Need for placing conducting coatings on insulating materials is virtually eliminated. It has wide ranges of applications both in industry and research. In addition, all the films have good stoichiometric properties. This indicates the strong incorporation of acids in the host PANI, which is in good accordance with our XRD and FE-SEM results. Moreover, the oxygen content is almost stable after incorporating the acids.

4.6. Electrical conductivity

4.6.1. Two probe method

Fig. 9. Spectacles the Two probe setup used 0.3M pristine PANI triturate with dissimilar four acids. In the two probe method the samples were pressed in to disks of 13 mm in diameter and about 1.5 mm in thickness under a pressure of 120 kg/cm². The resistance of the materials was measured by a Two – probe method with a digital multimeter (Keithley 6517B electrometer). The resistance was calculated on the basis of the average value of three different pellets.

4.6.2. Keithley 6517b electrometer

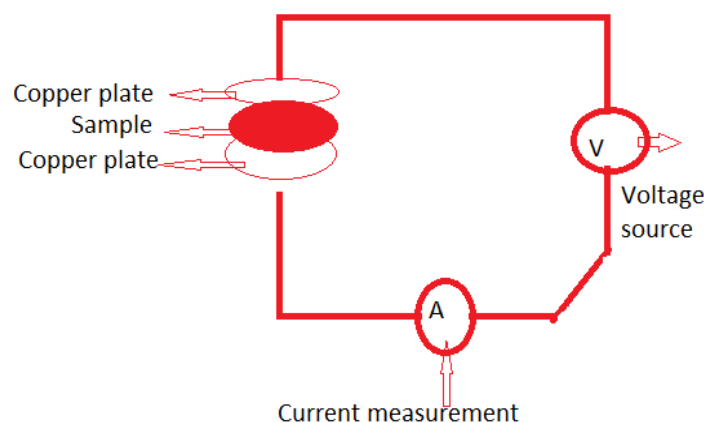


Fig. 9. Spectacles the Two probe setup for 0.3M pristine PANI triturate with dissimilar four acids

The Conductivity value of PANI with A, H, N, S increased on increasing the concentration of ammonium persulfate and then decreased with further increasing the concentration. Conductivity of PANI with A, H, N, and S was found to be nearly the same with reaction time. Conductivity of PANI with A, H, N, S prepared at room temperature (1.3×10^{-3} S/cm) was found to be higher than that of the PANI with A, H, N, S prepared at high temperature. Conductivity of polyaniline salts was found to be nearly the same (5.9×10^{-5} to 1.6×10^{-4} S/cm) with the reaction temperature (50 to 90° C). However, the conductivity was decreased drastically to 1×10^{-8} S/cm at 100° C. The effect of decrease in conductivity with increase in temperature may be due to over-oxidation process or the kinetic effects were favored in the oxidation of aniline. This is in good agreement with a previous report in the literature [72].

Fig. 10. Shows the temperature-dependent I–V characteristics of different acids used to fabricate (A, H, N and S) with 0.3 M of PANI nanoparticles. The current values were measured as a function of temperature (30–150 °C) by applying constant voltage ranging from 10 to 100 V (step of 10 V). The electrical conductivity of all the four samples has been determined in the temperature range from 303 K to 373 K. In all cases conductivity increases rise in temperature in the whole range, this is the characteristic of semiconducting behaviour [73, 74].

All the samples reveal a better response with temperature and voltage. Particularly higher current values are obtained at 150 °C than at other temperatures, which is evident from Fig. 10. Acidic acid used PANI showed a r of $2.8 \times 10^8 \Omega \text{ cm}$, which was found to decrease linearly ($r = 5.5 \times 10^7 \Omega \text{ cm}$) while adding HCL into the PANI matrix. This is attributed to the increase in the crystallite size of the HCL-PANI nanoparticles. In fact, the grain boundaries and the crystal lattice deficiency of the samples were reduced along with the increased adding different acids and measuring temperature. This would considerably reduce the r of the samples and improve the mobility of the charge carriers in it. Interestingly, a similar trend was observed by Mukherjee et al. s, the device allows electrical current to flow easily only in one direction, or as an ohmic contact, which can pass current in either direction with a negligibly small voltage drop. We can use this interface to form many useful devices. The temperature dependency of the electrical conductivity is characteristic of granuloose metals (strappingly higgledy-piggledy inhomogeneous coordination [75].

The current values were measured at different applied voltages from 1-10 V. The DC electrical conductivity (σ) for pristine PANI powder was calculated using the given equation 6:

$$\sigma = \frac{I}{V} \times \frac{d}{A} \quad (6)$$

Where, I = current, V = applied voltage, d = inter-probe distance, A = cross sectional area of the sample. The DC electrical conductivity of the prepared pristine polyaniline was measured using Keithley electrometer by applying voltage 1-10 V. The conductivity of the samples was deliberate using a two-probe method as a function of the temperature range from 303 to 393 K. Fig. 10. Shows the I-V characterization for pristine polyaniline prepared by various additives such as HCl, acetic acid, nitric acid and sulfuric acid. The electrical conductivity and activation energy of pristine polyaniline was calculated by following the equations (7), (8).

$$\sigma_{dc} = \frac{t}{RA} \quad (7)$$

$$\sigma = \sigma_0 \exp \left[\frac{-E_a}{k_B T} \right] \quad (8)$$

where t = Thickness of the pellet in cm; A = Area of the pellet in cm; R = Resistance of the pellet in Ω . k_B , σ , σ_0 , E_a and T is the thickness, resistance, active area, Boltzmann constant, conductivity, pre-exponential factor, activation energy and temperature, respectively. As seen from Fig. 10, the current values are increased with the increase. Compared to other nanoparticles, the HCL-PANI recorded the minimum activation energy of $E_a = 0.0389$ eV. As the guest atoms HCL are incorporated into the host PANI, a redistribution of energy levels especially with respect to the Fermi level takes place, which in turn decides the activation energy and conductivity. Moreover, the Vogel–Tamman–Fulcher and Mott’s three-dimensional variable range hopping mechanism can explain the non-Arrhenius behaviour. From the conductivity results, we conclude that the nanoporous: HCL-PANI nanoparticles are highly appropriate for the interfacial layer in MPS diodes to improve the device performance.

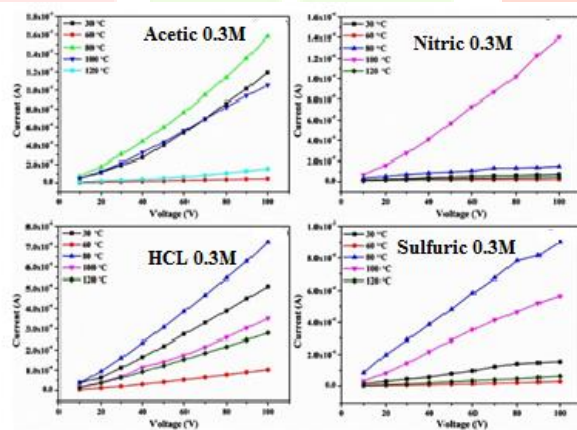


Fig. 10. Spectacles the temperature-dependent I–V characteristics of 0.3M pristine PANI triturate with dissimilar four acids

We found that on increasing the different acids (A, H, N and S) with 0.3 M of PANI nanoparticles, the experimental electrical conductivity of the PANI nanoparticles improved linearly. The acids adding samples with HCL of PANI recorded a maximum conductivity of $\sigma_{dc} = 4.4 \times 10^{-8} \text{ S cm}^{-1}$ (Table - 4). This is due to the decrease in the scattering along the grain-boundary and increase in the oxygen vacancies of the PANI samples. In addition, the incorporated HCL ions/atoms might increase the rate of volume required for ionic carriers to drift in the host PANI. This can improve the ionic mobility in the adding of samples to have enhanced conductivity [76].

Interestingly, this behaviour is well supported by the fact that the increasing crystallinity of the films can evidently decrease the charge transfer resistance during the double injection or ejection of ions and electrons, leading to an enhanced electrical conductivity [77]. Moreover, a sample with larger pores will have a good bonded structure, which can have an impact on the recorded values as per the studies by Zhu Ke and Cuevas et al. The obtained conductivity (10^{-13} – $10^{-15} \text{ S cm}^{-1}$) suggested a nearly conducting nature of the PANI nanoparticles. Indeed, all our prepared nanoparticles will be ideal and suitable to act as a polymer layer in MPS type SBDs to improve their performance [77].

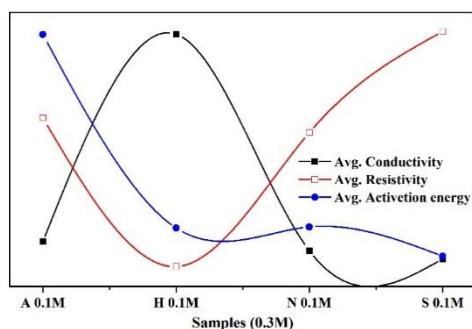


Fig. 11. Spectacles the Activation energy of 0.3M pristine PANI tritrate

Activation energy is the most important factor to analyze the electrical properties of the acids-PANI nanoparticles. Herein, Fig. 11. The calculated activation energy is found to decrease slowly on adding different acids as shown.

Fig. 12. Exhibits the Arrhenius plot of $1/T$ (K^{-1}) vs. $\ln(s)$ for different acids PANI nanoparticles. It is clearly seen from the Arrhenius plot that the calculated $\ln(s)$ values of all films seem to increase slowly with $1/T$ (K^{-1}). Improved $\ln(s)$ at higher temperature is a fact that the independent charge carriers might hop from one localized state to another state due to the increase in their free volume and segmental mobility at suitable temperature.

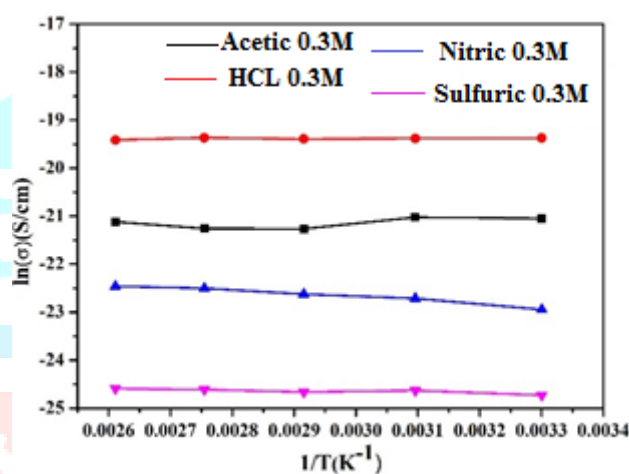


Fig. 12. Spectacles the Arrhenius plot of $1/T$ (K^{-1}) vs. $\ln(s)$ for 0.3M pristine PANI tritrate with dissimilar four acids

The resistivity of the PANI was calculated using the equation (9).

$$\rho = \frac{RA}{l} \quad (9)$$

4.1. Tabularization

Electrical parameters of pristine PANI tritrate with dissimilar four acids

Samples	Conductivity (S/cm)	σ_{dc}	Resistivity ρ (Ω/cm)	Activation energy (Ea) (eV)
A 0.3M	7.355×10^{-7}		2.864×10^8	0.25096
H 0.3M	4.1446×10^{-5}		5.569×10^7	0.0389
N 0.3M	5.8322×10^{-7}		2.636×10^8	0.04002
S 0.3M	4.5058×10^{-6}		4.205×10^8	0.00808

4.6.3. Fabrication of Cu/PANI/n-Si (MPS) Type Schottky Barrier Diodes

The diode parameters such as n and Φ_B of the fabricated Cu/PANI/p-Si diodes were analysed at light intensity using portable solar simulator (PEC-L01). Currently, the Schottky diode consumes been momentarily reconnoitred through commissioning changeover metal dichalcogenides, since of their prospective character in differentiated application in devices. The Schottky diode is a persuasive machinery that is in employment in the manufacturing and theoretical arenas of voluminous microelectronics in addition photovoltaic strategies. Stimulatingly, HCL have countless noticeable topographies comparable band gap, high optical absorption, and encrusted variety of prearrangement in the middle of the cations. These belongings expedite them in the direction of remain an imperative contender in the chemical oxidative method. This is reasonably vindicated as PANI is known to be p-type measureable and Si as n-type. The heavyweight incapacitating consequences in fragmented band gap, someplace conduction band electron circumstances on the n-side are supplementary or less associated with valence band hole federations on the p-side. Consequently under forward bias, as voltage commences to intensification, electrons tunnel concluded the appropriate constricted barrier.

As voltage intensifications additional electron- hole states turn out to be additional skewed and the current droplets, this is called negative resistance because current reductions with accumulative voltage. As voltage increases still further, the diode commences to manoeuvre as a schotty diode, where electrons portable by conduction transversely the dielectric and no elongated by tunnelling through the schotty barrier. For the tunnelling fragment is weedy outstanding to subordinate concentration of n-type material as demonstrated by Esaki diode. The schotty barrier diode also illustrations nonlinear comporment together in shadowy as well as under luminescent illumination. Current worth is appreciated to heighten multifarious on light illumination as associated to that under dark. Both I_D and I_{ph} conduction mechanism of the Cu/PANI/n-Si diode was described by thermionic emission theory (TET) using the following equation (10) [78].

$$J = J_0 \exp \left[\frac{qV}{nk_B T} - 1 \right] \quad (10)$$

Where J_0 is the reverse leakage current density, q is the electron charge, V is the applied voltage, n is the ideality factor, k_B is the Boltzmann constant and T is the absolute temperature. The semi-logarithmic plot of current density ($\ln J$) versus voltage (V) is displayed in the Fig. 13 and equation 11.

$$n = \frac{q}{(K_B T)} \frac{dV}{(d(\ln J))} \quad (11)$$

Ideality factor was Finding from this eqn n is the ideality factor, k_B is the Boltzmann constant and T is the absolute temperature. The semi-logarithmic plot of current density ($\ln J$), q is the electron charge, V is the applied voltage.

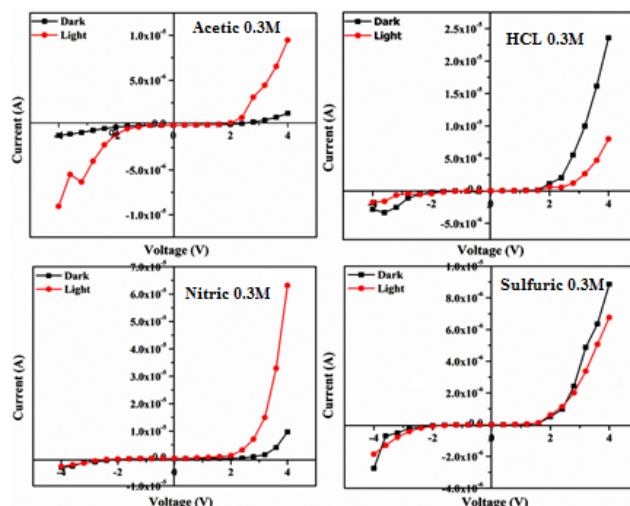


Fig. 13. Spectacles The I-V Characteristics of MPS type SBDs using 0.3M pristine PANI triturate with dissimilar

four acids

$$(\Phi_B) = \frac{(k_B T)}{q} \ln \left[\frac{A A^* T^2}{J_0} \right] \quad (12)$$

Where, Φ_B is the barrier height, A^* is the effective Richardson constant for p-type Si, k_B is the Boltzmann constant and T is the absolute temperature. The semi-logarithmic plot of current density ($\ln J$), q is the electron charge, J_0 is the reverse leakage current density. Equation 12. Used to calculate the barrier height (Φ_B).

The Φ_B and n prices were summarized in (Table - 5). From this Table, hefty n values were achieved in the ailment of together in darkness and under the light condition for S of PANI content on SBDs. The effective Schottky barrier heights (SBHs) and ideality factors conquered since the current–voltage (I–V) characteristics devour fluctuated from diode to diode. The minimum ideality factor ($n = 2.16$) with corresponding barrier height ($\Phi_B = 0.56$) value obtained for H of Cu/PANI/n-Si diode is under the light illumination circumstance. Moreover, it increases to 3.11 in darkness. It may be due to the formation of oxygen deficiency in the pristine polyaniline. From these results, all the pristine polyaniline exhibit the semi-conducting nature [79 – 81].

The recital and reliability of Schottky barrier diodes (SBDs) are significantly pertinent with the crossing point layer choice for both metal- insulator-semiconductor (MIS) and metal doped polymer semi- conductor (MPS) types SBDs [82 - 85].

The downward curve in curvature region (non-ideal behaviour) of the forward bias I-V plots at a sufficiently huge voltage has an aspect to the presence of not statistically significant, which equilibrates with the semiconductor, apart from the R_s effect of non-aligned region in the Schottky barrier diode [86 - 90]. The current transport mechanism of Cu/PANI/n-Si SBDs was explained by thermionic emission (TE) theory based on the condition ($V > 3kT/q$). According to this theory [91, 92], the current density (J) of MPS type SBDs was calculated using eqn 4.

The current–voltage (I–V) measurement under dark and light conditions explores the photodetector properties and performance of the fabricated device. Fig. 10. Displays the I–V characteristics of the Cu/PANI/p-Si SBDs measured under dark and light conditions with 0.03M of different acids (A, H, N and S) based polymer layer. The forward and reverse current values of the MPS diode were measured by applying a constant bias voltage ranging from +4 V to -4 V with a Keithley electrometer. The measuring parameters of the fabricated MPS SBDs under dark and light conditions using a portable solar simulator (PEC-L01) have been reported in our previous work. The diode measured under light conditions exhibits higher current values than under the dark conditions Fig. 13. This behaviour outcome indicates that all the Cu/PANI/p-Si diodes are highly photo-conducting in nature. In particular, the diode fabricated with HCL shows higher current values (mA level) when compared to other diodes Fig. 13.

The semi-logarithmic plot of the MPS diode is shown in Fig. 14. The ideality factor (n) of the diodes was found to reduce steeply under dark conditions on increasing the different acids with PANI (Table 5). Compared to the dark conditions, the diodes measured under light conditions revealed lower n values. This is mainly due to the increase in the photo-generated charge carriers (e^-h^+) along with the improved conversion efficiency of the semiconductor layer and absorption of interfacial layer. However, the HCL MPS diode shows a higher ideality factor of under light conditions compared to that under dark conditions. This may be ascribed to the generation of a smaller amount of e^-h^+ pairs and their recombination. The MPS SBDs fabricated with HCL-PANI obtained a lower ideality factor in particular under light conditions. Generally, the deviation of the ideality factor from the ideal value is because of the presence of a large number of trapping states. Also, a higher n value is sometimes observed in the hetero-structures of two different materials due to the large lattice mismatch.

The estimated barrier height (Φ_B) was found to vary from 0.75 to 0.60 eV with different acids. In fact, the potential variation across the thin interfacial layer and the effect of interface states with applied voltage are the main reasons for the changes in the barrier height (Φ_B) of the diode, which has been analyzed by Turut et al. From the Cu/PANI/p-Si diode results, we observed that the presence of HCL used PANI in between the metal and semiconductor interface strongly enhanced the photo-diode parameters, particularly, the MPS diode fabricated with HCL-PANI, which suggests that the promising potential for MPS type diode applications. However, there are only a few studies on polymer-based SBDs with organic/polymer interfacial layers, which are known as metal polymer semi- conductor (MPS) type SBDs [93]. The decreasing of the Schottky barrier height by image forces and thermionic field emission at the interface state are explained by the acid level dependence of PANI samples [94]. The prepared Cu/PANI/n- Si SBDs express a good photo-conducting nature [95, 96].

4.2. Tabularization

Cu/PANI/n- Si preparation of MPS type SBDs using 0.3M pristine PANI tritrate with dissimilar four acids

Samples	Barrier height (Φ_B) (eV)		Ideality factor (n)	
	Dark	Light	Dark	Light
A 0.3M	0.7	0.75	2.9	3.11
H 0.3M	0.58	0.56	3.08	2.16
N 0.3M	0.69	0.68	5.44	4.35
S 0.3M	0.61	0.60	3.79	8.74

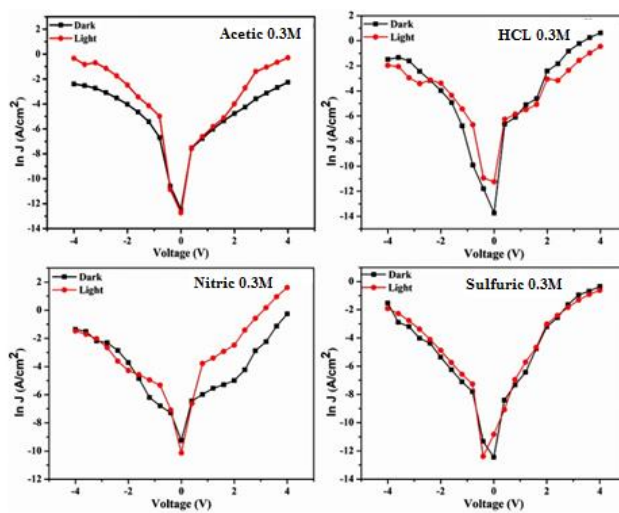


Fig. 14. Spectacles the semi-logarithmic plot of MPS type SBDs using 0.3M pristine PANI tritrate with dissimilar four acids

5. CONCLUSIONS

In this paper, we attempt to consolidate the important milestones in the development of polymer based schottky barrier diodes by reviewing the major works on fabrication, characterization. The main apprehension of conjugated polymer ingredients is the obtainment of exceedingly well-organized crystalline structures. This necessitates a methodical mechanism of the polymer macromolecular structural design. Synthetically, the monomers are primary accompanying in a unvarying method to kowtow to unbending main manacles. These chains are formerly connected and crammed in unit cells systematized into crystallites. They are additional weighted into unvarying collections establishing thin layers. Undeniably, a methodical sample is the one consuming not individual sophisticated crystallinity but then again correspondingly consistency or anisotropy that customarily retains a developed grade of molecular gathering and positioning. The studies obtainable in this paper stand an endeavour to reconnoitre the opportunity of procurement methodical thin films or conjugated polymers, using surfactant assemblages in micellar and micro suspension mass media. Pristine PANI efficaciously completed with help of the chemical oxidative method by the unpretentious and low-cost performance at dissimilar acids Acetic, HCL, Nitric, and Sulfuric. FTIR spectroscopy imitates the long-established by the benzoid and quinoid rings lengthening. XRD investigation long-established the amorphous nature. FE-SEM images publicized the interconnected complex smidgeons with the indiscriminately concerned with superficial for the PANI. The premeditated E_g values remained originate to wide-ranging from 3.2 to 3.6 eV. The DC electrical conductivity results confirm the semiconducting behaviour of the samples. Cu/PANI/p-Si (MPS) type of tremendous light rejoinder is underwritten by the PANI which are acknowledged for their optical movement. So, here also, coalescing consequence of the four concentration in the composite of the PANI is in performance momentous protagonist. These are HCL, acetic, nitric, and sulfuric. The perfection of this taxonomy scrutiny is prolonged by means of using silicon n-type layer in the Schottky diode for humanising their presentation. Auxiliary, the diode considerations such as ideality factor (n), barrier height (ϕ_B) and reverse saturation current (I_0) remained premeditated and deliberated. Furthermore, the middling electrical conductivity of the sample intensifications and triggering energy shrinkages with the intensification in substrate temperature. The pellets deposited at 500 °C manufactured the maximum average electrical conductivity of $\sigma_{dc} = 0.54 \times 10^{-4}$ S/cm and their corresponding activation energy is 0.092 eV. From Cu/PANI/p-Si (MPS) type SBDs,

the experimental results of forward and reverse biased I-V characteristics exposed the improved barrier height (Φ_B) and reduced ideality factor (n) values for higher device temperature. Paralleled with other SBDs, we demonstrated that the device fabricated at 400 °C yielded the minimum average ideality factor tabularized value.

6. References

- [1] Tang CW, van Slyke SA. Organic electroluminescent diodes. *Appl Phys Lett* 1987;51:913–5.
- [2] Burrougher JH, Bradley DDC, Brown AR, Marks RN, Mackey K, Friend RH, et al. Light emitting diodes based on conjugated polymers. *Nature* 1990;347:539–41.
- [3] Lin Y-Y, Gundlach DJ, Nelson SF, Jackson TN. Penta- cene-based organic thin-film transistors. *IEEE Trans Elec- tron Dev* 1997; 44(8):1325–31.
- [4] Dodabalapur A, Katz HE, Torsi L, Haddon RC. Organic heterostructure field-effect transistors. *Science* 1995; 269: 1560–2.
- [5] D. Li, J. X. Huang, and R. B. Kaner, “Polyaniline nanofibers: a unique polymer nanostructure for versatile applications,” *Accounts of Chemical Research*, vol. 42, pp. 135–145, 2009.
- [6] M. Khalid, J. J. S. Acuña, M. A. Tumelero, J. A. Fischer, V. Zoldan, and A. A. Pasa, “Sulfonated porphyrin doped polyaniline nanotubes and nanofibers: synthesis and characterization,” *Journal of Materials Chemistry*, vol. 22, pp. 11340–11346, 2012.
- [7] K.M. Molapo, P.M. Ndingili, R.F. Ajayi, G. Mbambisa, S.M. Mailu, N. Njomo, M. Masikini, P. Baker and E.I. Iwuoha, *Int. J. Electrochem. Sci.*, 7, 11859 (2012). Vol. 31, No. 12 (2019).
- [8] S. Bocchini, A. Chiolerio, S. Porro, D. Accardo, N. Garino, K. Bejtka, D. Perrone and C. Pirri, *J. Mater. Chem. C*, 1, 5101 (2013); <https://doi.org/10.1039/c3tc30764f>.
- [9] A. Chiolerio, S. Bocchini and S. Porro, *Adv. Funct. Mater.*, 24, 3472 (2014); <https://doi.org/10.1002/adfm.201470147>.
- [10] B.W.J.E. Beek, L.H. Slooff, M.N. Wienk, J.M. Kroon and R.A.J. Janseen, *Adv. Funct. Mater.*, 15, 1703 (2005); <https://doi.org/10.1002/adfm.200500201>.
- [11] X.M. Sui, C.L. Shao and Y.C. Liu, *Appl. Phys. Lett.*, 87, 113115 (2005); <https://doi.org/10.1063/1.2048808>.
- [12] M. Khalid and F. Mohammad, “Preparation, FTIR spectroscopic characterization and isothermal stability of differently doped fibrous conducting polymers based on polyaniline and nylon-6, 6,” *Synthetic Metals*, vol. 159, pp. 119–122, 2009.
- [13] A. A. Khan and M. Khalid, “Preparation, FTIR spectroscopic characterization and isothermal stability of differently doped conductive fibers based on polyaniline and polyacrylonitrile,” *Synthetic Metals*, vol. 160, no. 7-8, pp. 708–712, 2010.
- [14] L. Zhang, H. Peng, J. Sui, P. A. Kilmartin, and J. Travas-Sejdic, “Polyaniline nanotubes doped with polymeric acids,” *Current Applied Physics*, vol. 8, no. 3-4, pp. 312–315, 2008.
- [15] Q. Yao, L. D. Chen, W. Q. Zhang, S. C. Liufu, and X. H. Chen, “Enhanced thermoelectric performance of single-walled carbon nanotubes/polyaniline hybrid nanocomposites,” *ACS Nano*, vol. 4, no. 4, pp. 2445–2451, 2010.
- [16] R. Sainz, W. R. Small, N. A. Young et al., “Synthesis and properties of optically active polyaniline carbon nanotube composites,” *Macromolecules*, vol. 39, no. 21, pp. 7324–7332, 2006.
- [17] X. T. Zhang, W. H. Song, P. J. F. Harris, G. R. Mitchell, T. T. T. Bui, and A. F. Drake, “Chiral polymer-carbon-nanotube composite nanofibers,” *Advanced Materials*, vol. 19, no. 8, pp. 1079–1083, 2007.
- [18] Y. Zhou, Z.-Y. Qin, L. Li et al., “Polyaniline/multi-walled carbon nanotube composites with core-shell structures as supercapacitor electrode materials,” *Electrochimica Acta*, vol. 55, no. 12, pp. 3904–3908, 2010.
- [19] G. M. Spinks, V. Mottaghitlab, M. Bahrami-Samani, P. G. Whitten, and G. G. Wallace, “Carbon-nanotube-reinforced polyaniline fibers for high-strength artificial muscles,” *Advanced Materials*, vol. 18, no. 5, pp. 637–640, 2006.
- [20] A. L. Cabezas, Z. B. Zhang, L. R. Zheng, and S. L. Zhang, “Morphological development of nanofibrillar composites of polyaniline and carbon nanotubes,” *Synthetic Metals*, vol. 160, pp. 664–668, 2010.
- [21] J.-Q. Dong and Q. J. Shen, “Enhancement in solubility and conductivity of polyaniline with lignosulfonate modified carbon nanotube,” *Journal of Polymer Science B*, vol. 47, no. 20, pp. 2036–2046, 2009.
- [22] P. Jimenez, W. K. Maser, P. Castell, M. T. Martínez, and A. M. Benito, “Nanofibrillar polyaniline: direct route to Carbon nanotube water dispersions of high concentration,” *Macromolecular Rapid Communications*, vol. 30, pp. 418–422, 2009.
- [23] P. Jimenez, P. Castell, R. Sainz et al., “Carbon nanotube effect on polyaniline morphology in water dispersible composites,” *The Journal of Physical Chemistry B*, vol. 114, pp. 1579–1585, 2010.
- [24] R. Sainz, A. M. Benito, M. T. Martínez et al., “Soluble self-aligned carbon nanotube/polyaniline composites,” *Advanced Materials*, vol. 17, no. 3, pp. 278–281, 2005.
- [25] M. Ginic-Markovic, J. G. Matisons, R. Cervini, G. P. Simon, and P. M. Fredericks, “Synthesis of new polyaniline/nanotube composites using ultrasonically initiated emulsion polymerization,” *Chemistry of Materials*, vol. 18, no. 26, pp. 6258–6265, 2006.
- [26] D. Normile, “Nanotubes generate full-color displays,” *Science*, vol. 286, no. 5447, pp. 2056–2057, 1999.
- [27] J. Kong, N. R. Franklin, C. W. Zhou et al., “Nanotube molecular wires as chemical sensors,” *Science*, vol. 287, no. 5453, pp. 622–625, 2000.
- [28] C. R. Martin, “Nanomaterials: a membrane-based synthetic approach,” *Science*, vol. 266, no. 5193, pp. 1961–1966, 1994.
- [29] J. Huang and M. X. Wan, “In situ doping polymerization of polyaniline microtubules in the presence of β -naphthalenesulfonic acid,” *Journal of Polymer Science A*, vol. 37, no. 2, pp. 151–157, 1999.
- [30] L. Zhang, H. Peng, P. A. Kilmartin, C. Soeller, and J. Travas-Sejdic, “Polymeric acid doped polyaniline nanotubes for oligonucleotide sensors,” *Electroanalysis*, vol. 19, no. 7-8, pp. 870–875, 2007.
- [31] Novak BM. *Adv. Mater.* 1993; 5: 422.
- [32] Bian C and Xue G. *Mat. Lett.* 2007; 61: 1299.
- [33] Gupta R, Misra SCK, Malhotra BD, Beladakere NN, Chandra S. Metal/semiconductive polymer Schottky de- vice. *Appl Phys Lett* 1991;58:51.
- [34] Aernouts T, Geens W, Poortmans J, Nijs J, Mertens R. Analysis and simulation of the IV -characteristics of PPV- oligomer based Schottky diodes. *Synth Met* 2001; 122: 153–5.
- [35] Turut A, K€ooleliF. Semiconductive polymer-based Schotky diode. *J Appl Phys* 1992;72:818.

- [36] shoba E, pasupathy N, thirunavukkarasu P, chandrasekaran J, parthasarathy G, Syn of MPS Diode Using Polyaniline by COM and its Temperature Dependent Electrical Conductivity Behaviour, Asian Journ of chem, 12 (2019), 2846-2854, <https://doi.org/10.14233/ajchem.2019.22143>.
- [37] M. Balaji, J. Chandrasekaran, M. Raja, S. Rajesh Structural, J. Mater. Sci. Mater. Electron. 27, 11646 (2016).
- [38] I. Sapurina and J. Stejskal, Polym. Int. 57, 1295 (2008).
- [39] I. Sapurina and J. Stejskal, Russ. J. Gen. Chem. 82, 256 (2012).
- [40] J. Stejskal, I. Sapurina, M. Trchov'a, and E. N. Konyushenko, Macromolecules 41, 3530 (2008).
- [41] H. Valentov'a, J. Proke's, J. Nedbal, and J. Stejskal, Chem. Pap. 67, 1109 (2013).
- [42] S. Fedorova and J. Stejskal, Langmuir 18, 5630 (2002).
- [43] J. Stejskal, P. Kratochv'íl, S. P. Armes, S. F. Lascelles, A. Riede, M. Helmstedt, J. Proke's, and I. K'rivka, Macromolecules 29, 6814 (1996).
- [44] G. 'Ciri'c-Marjanovi'c, Synth. Met. 170, 31 (2013).
- [45] J. Stejskal, Chem. Pap. 67, 814 (2013).
- [46] V. Babayan, N. E. Kazantseva, I. Sapurina, R. Mou'cka, J. Vil'c'akov'a, and J. Stejskal, Appl. Surf. Sci. 258, 7707 (2012).
- [47] P. Bober, J. Stejskal, M. 'Sp'rkov'a, M. Trchov'a, M. Varga, and J. Proke's, Synth. Met. 160, 2596 (2010).
- [48] J. A. Marins and B. G. Soares, Synth. Met. 162, 2087.
- [49] J. Tokarsk'y, L. Kulh'ankov'a, V. St'yskala, K. Mamulov'a Kutl'akov'a, L. Neuwirthov'a, V. Mat'ejka, and P. 'Capkov'a, Appl. Clay Sci. 80-81, 126 (2013).
- [50] J. Stejskal, J. Polym. Mater. 18, 225 (2001).
- [51] J. Stejskal, and I. Sapurina, Pure Appl. Chem. 77, 815 (2005).
- [52] K. Crowley, M. R. Smyth, A. J. Killard, and A. Morrin, Chem. Pap. 67, 771 (2013).
- [53] Y. Wang, N. Herron, J Phys. Chem. 95 (1991) 525.
- [54] S. Karuppuchamy, J. M. Jeong, J Oleo. Sci. 55 (2006) 263.
- [55] W. Sugimoto, H. Iwata, Y. Murakami, Y. Takasu, J Electrochem. Soc. 151 (2004) A1181.
- [56] P. S. Rao, J. Anand, S. Palaniappan, D. N. Sathyanarayana, European Polymer Journal 36 (2000) 915.
- [57] S. B. Kulkarni, S. S. Joshi, C. D. Lokhande, Chem. Eng. J. 166 (2011) 1179.
- [58] S. Ramanathan, V. Ponnuswamy, B. Gowtham, K. Premnazeer, and S. C. Murugave J Opto and Adv Mater 16, (2014)
- [59] G. Pradeesh V. Ponnuswamy J. Chandrasekaran B. Gowtham and S. Ashokan J Mater Sci: Mater Electron <https://doi.org/10.1007/s10854-017-7663-2>.
- [60] J.A. Khan, M. Qasim, B.R. Singh, S. Singh, M. Shoeb, W.Khan, D. Das, A.H. Naqvi, Spectrochim. Acta A 109, 313 (2013).
- [61] U.S. Sharma, R. Shah, AIP Conference Proceedings vol. 1728, p. 020275, (2016). doi:10.1063/1.4946326.
- [62] L.M. Irimpan, Spectral and nonlinear optical characterization of ZnO nanocomposites. Cochin University of Science and Technology. Ph.D Thesis (2008).
- [63] D.M. Mohilner, R.N. Adams and W.J. Argersinger, J. Am. Chem. Soc., 84, 3618 (1962); <https://doi.org/10.1021/ja00878a003>.
- [64] N. Gospodinova, L. Terlemezyan, P. Mokeva and K. Kossev, Polymer, 34, 24334 (1993).
- [65] R.K. Mishra, P.P. Sahay, Mater. Res. Bull. 47, 4112 (2012).
- [66] H.M. Shanshool, M. Yahaya, W.M. Mat Yunus, I.Y. Abdullah, J. Mater Sci. 27, 9804 (2016).
- [67] M.A.R.H. El-Zahed, A. El-Korashy, Effect of heat treatment on some of the optical parameters of Cu₉Ge₁₁Te₈₀ films. Vacuum 68, 19 (2003).
- [68] R. Suresh, V. Ponnuswamy, R. Mariappan, Appl. Surf. Sci. 273, 457 (2013).
- [69] S.S. Ray and M. Biswas, Synth. Met., 108, 234 (2000); [https://doi.org/10.1016/S0379-6779\(99\)00258-1](https://doi.org/10.1016/S0379-6779(99)00258-1).
- [70] Senthilkumar, Subramanian, and Annamalai Rajendran. MOJ Poly. Sci 1: 31. (2017) <https://doi.org/10.15406/mojps.2017.01.00031>.
- [71] Hu F, Li W, Zhang J, and Meng W. J Mater Sci: Mater Electron 30 321-327(2014). <https://doi.org/10.1016/j.jmst.2013.10.009>.
- [72] Appel, G.; Yfantis, A.; Gopel, W.; Schmeiber, D. Synth. Met. 1996, 83, 197-200.
- [73] G. B. V. S. Lakshmi, Vazid Ali, Pawan Kulriya, Azher M. Siddiqui, M. Husain, M. Zulfequar, Physica B, 392, 259 (2007).
- [74] Sadiya Ameen, Vazid Ali, Zulfequar, M. Mazhrul Haq, M. Husain, Physica B, 403, 2861 (2008).
- [75] J.C.Scott, S.A.Carter, S.Karg and M.Angelopoulos // Synthetic Metals 87 (1997) 1197.
- [76] S.M. Sze, (2nd edn.) Semiconductor Devices. (Wiley New York, 2001) p. 224.
- [77] L.R. Canfield, R. Vest, T.N. Woods, R. Korde, Ultrav. Technol. V 31, 2282 (1994).
- [78] B. Keskin, C. Denktas, A. Altindal, U. Avciata, A. Gul, Polyhedron 38, 121 (2012).
- [79] R. Patil, A.S. Roy, K.R. Anilkumar, K.M. Jadhav and S. Ekhelkar, Composites: Part B, 43, 3406 (2012); <https://doi.org/10.1016/j.compositesb.2012.01.090>.
- [80] E. Erem, M. Karaksha and M. Sacak, Eur. Polym. J., 40, 785 (2004); <https://doi.org/10.1016/j.eurpolymj.2003.12.007>.
- [81] H. Tange, A. Kitani and M. Shiotani, Electrochim. Acta, 41, 1561(1996); [https://doi.org/10.1016/0013-4686\(95\)00408-4](https://doi.org/10.1016/0013-4686(95)00408-4).
- [82] A. Gok and B. Sari, J. Appl. Polym. Sci., 84, 1993 (2002); <https://doi.org/10.1002/app.10487>.
- [83] T.T.A. Tuan, D.H. Kuo, C.C. Li and W.C. Yen, J. Mater. Sci. Mater. Electron., 25, 3264 (2014); <https://doi.org/10.1007/s10854-014-2012-1>.
- [84] H. Tecimer, A. Turut, H. Uslu, S. Altindal and I. Uslu, Sens. Actuators A Phys., (2013); <https://doi.org/10.1016/j.sna.2013.05.027>.
- [85] J. Werner and H. Guttler, J. Appl. Phys., 69, 1522 (1991); <https://doi.org/10.1063/1.347243>. 1561 (1996);
- [86] O. Cicek, H. UsluTecimer, S.O. Tan, H. Tecimer, I. Orak and S. Altindal, Compos. Part B Eng., 113, 14 (2017) <https://doi.org/10.1016/j.compositesb.2017.01.012>.
- [87] S. Altindal, S. Karadeniz, N. Tugluoglu and A. Tataroglu, Solid-State Electron., 47, 1847 (2003); [https://doi.org/10.1016/S0038-1101\(03\)00182-5](https://doi.org/10.1016/S0038-1101(03)00182-5).
- [88] J.H. Werner and H.H. Guttler, J. Appl. Phys., 69 1522 (1991); <https://doi.org/10.1063/1.347243>.
- [89] N. Tugluoglu, S. Karadeniz and S. Altindal, Appl. Surf. Sci., 239, 481 (2005); <https://doi.org/10.1016/j.apsusc.2004.06.015>.
- [90] P. Chattopadhyay, Solid-State Electron., 37, 1759 (1994); [https://doi.org/10.1016/0038-1101\(94\)90223-2](https://doi.org/10.1016/0038-1101(94)90223-2).
- [91] S. Mahendia, P.K. Goyal, A.K. Tomar, R.P. Chahal and S. Kumar, J. Electron. Mater., 45, 5418 (2016); <https://doi.org/10.1007/s11664-016-4677-0>.
- [92] E.H. Rhoderick and R.H. Williams, Metal-Semiconductor Contacts, Oxford: Clarendon, edn. 2 (1988).

- [93] R.F. Schmitsdorf, T.U. Kampen and W. Monch, Surf. Sci., 324, 249 (1995); [https://doi.org/10.1016/0039-6028\(94\)00791-8](https://doi.org/10.1016/0039-6028(94)00791-8).
- [94] F.C. Chiu, Adv. Mater. Sci. Eng. (2014). <https://doi.org/10.1155/2014/578168>.
- [95] N. Senthil kumar, M. Sethu Raman, J. Chandrasekaran, R. Priya, M. Chavali, R. Suresh, Mater. Sci. Semicond. Process. 41, 497 (2016).
- [96] M. Balaji, J. Chandrasekaran, M. Raja, S. Rajesh, J. Mater. Sci. Mater. Electron. 27, 11646 (2016).

